Reply to Referee #1

We thank the anonymous referee for the thoughtful comments that has resulted in changes that improved the quality of our manuscript. We provide responses to the referee comments (in **bold**) below and provide the additional citations at the end of this response:

A critical evaluation and assessment of what worked and what did not during the ARIAs campaign is missing in the present manuscript.

Upon revision we will add details about the goals of the ARIAs campaign and what was actually accomplished. In particular, the following text will be added towards the end of the Introduction of the revised manuscript:

> The ARIAs campaign was designed to characterize and quantify the composition of trace gases and aerosol optical properties over Hebei to improve tools used to evaluate the effectiveness of air pollution reduction policies. Since air pollution transport from Asia typically peaks in early to mid-spring (Liu et al., 2003), we hoped to provide detailed altitude profiles over the Asian source region to enable Lagrangian experiments with KORUS-AQ, but only two sustained transport events occurred (Peterson et al., 2019). Despite the infrequent transboundary pollution events, ARIAs observations generated valuable characteristic pollution signatures that helped describe combustion efficiency and its impact downwind (Halliday et al., 2019), to correct model biases of CO in global chemistry-climate models (Gaubert et al., 2020) and to show that MOPITT bias increases at high CO concentrations (Tang et al., 2020). Furthermore, ARIAs measurements characterized aerosol optical properties in the planetary boundary layer and free troposphere during clean and polluted conditions (Wang et al., 2018), as well as used in the validation of MAX-DOAS profiles of NO_2, SO_2, HONO, HCHO, CHOCHO, and aerosols (Wang et al., 2019b).

CO/CO2 ratio: How do the measurements of CO/CO2 compare to ground based measurements in urban centers of China? How do the CO/CO2 of the ARIAs study compare to measurements on other continents where pollution control measures have led to decreasing CO/CO2 ratios over time? How do the CO/CO2 ratios in plumes that are associated with biomass burning (Fig. 5a) compare to studies of biomass burning emission ratios? How many flights showed evidence of biomass burning emissions such as from past harvest residue burns?

We agree that it is important to investigate the CO/CO_2 ratios from ground-based observations. However, the ARIAs campaign did not include GHGs measurements at ground stations. We have to rely on the ratios from literature and the KORUS-AQ campaign to answer the referee's concern. If the referee is aware of available CO/CO_2 ratios from Hebei, a reference would be appreciated. We will add the table below to the main text comparing our ARIAs CO/CO_2 ratio to the literature and discuss these studies with the following new text to be added to Section 3.1:

> These measurements are illustrative of low-efficiency fossil fuel combustion, likely from residential coal burning as these observations were all collected at ~500 m, and are compared to other studies in Table 3. Our results indicating the prevalence of low-

> efficiency combustion agree with KORUS-AQ airborne data over the West Sea with 2.8% CO/CO_2 (Tang et al., 2018), as well as with December 2017 surface measurements at Jingdezhen station in central China of 2.6% when air mass transport was from northern China (Xia et al., 2020). Compared to earlier studies in rural and urban areas of Beijing in the mid-2000s (Han et al., 2009; Wang et al., 2010b) and to 2011 measurements in Nanjing (Huang et al., 2015), the ARIAs CO/CO_2 ratio is 0.1-2.7% lower, evident of some success of regional pollution control strategies. By contrast, our CO/CO_2 ratio is higher than satellite-derived ratios over megacities that have implemented extensive pollution control measures (Silva et al., 2013). Similarly, compared to airborne measurements from the 2015 Wintertime INvestigation of Transport, Emissions, and Reactivity (WINTER) campaign in the Baltimore/Washington, D.C. region (Ren et al., 2018), our CO/CO_2 ratio is about a factor of 6 larger.

When we went back to the data to identify the number of flights which sampled biomass burning plumes, we realized the 1-minute average data was missing some of these short events. We will instead use the 1-second data in Figure 5 in the revised manuscript to better show these plumes. The ARIAs CO/CO_2 ratios measured in plumes associated with biomass burning is ~6%. This ratio is comparable to past studies evaluating emission ratios from wheat straw burning in Hebei (Cao et al., 2008). We identified three ARIAs flights which briefly sampled biomass burning plumes. We will add these additional details with the following revised text to Section 3.1:

> Higher CO/CO_2 ratios (~6%) with less than 0.1 ppm SO_2, as seen briefly during three ARIAs flights, are more in line with emissions from burning of wheat straw in Hebei of ~6% (Cao et al., 2008), and other inefficient, biofuel combustion.

We will revise a sentence in the Conclusions to now read:

> Ratios of CO/CO_2 indicate inefficient combustion from residential coal and biomass burning throughout the region, but have decreased in China since the early 2000s suggesting the implementation of successful pollution control strategies.

We will add the following new table, which will be *Table 3* of the revised manuscript, in reply to this comment:

Study	**Location**	**Year**	**CO/CO_2 (%)**
This Study*	North China Plain	May-June 2016	3.1
Wang et al., 2010	Miyuan, rural Beijing	Winter 2004	5.8
		Winter 2008	3.8
Huang et al., 2015	Nanjing, China	2011	3.4-4.2
Silva et al., 2013	Space-based Megacities	June 2009-May 2010	Beijing/Tianjin: 4.3 Mumbai: 1.4 New York: 1.3 London: 0.6
Han et al., 2009	Beijing, China	2005-2006	Fall: 3.0 Winter: 4.4
Tang et al., 2018*	West Sea	May-June 2016	2.8

	Seoul		0.9
Xia et al., 2020	Jingdezhen station, central China, airflow from N China	December 2017	2.6
	Jingdezhen station, airflow from SW China	18-21 January 2017	1.4
Ren et al., 2018	Baltimore/Washington, D.C.	Winter 2016	0.53

*=Airborne studies

Hydrocarbon profiles: How do the hydrocarbon values and their enhancement ratios to CO measured during ARIAs compare to ground based measurements in metropolitan areas of China, Europe or the US? How do they compare to biomass burning profiles?

High concentrations of anthropogenic VOCs measured during ARIAs suggest that our flights are close to local VOCs sources, however we find that very few VOCs species exhibit a strong correlation with CO. Since CO is a marker of combustion, the lack of correlation indicates the lack of common source signatures and/or some photochemical aging of the sampled airmasses. For these reasons, we plan to add another column to Table S2 reporting the VOC/CO ratio where R>0.50 for 13 VOCs. In general, hydrocarbon enhancement to CO during ARIAs are lower than other metropolitan ground-based studies.

The following new text will be added to Section 3.2:

> Since CO can be marker for anthropogenically emitted hydrocarbons, particularly combustion products, we first use the ratios of various VOCs to CO to reveal insight into changes in emissions in the region. Ratios of VOCs to CO can vary substantially among cities (Baker et al., 2008; Warneke et al., 2007), but in general can provide details about fuel types and combustion efficiency between metropolitan regions. Despite ARIAs measurements sampling in close proximity to local VOCs sources, most VOCs do not correlate strongly with CO, reflective of the lack of common source signatures and some photochemical aging of the sampled airmasses. We report slopes of VOCs/CO in Table S2 when R>0.50. Ethane has the strongest correlation with CO (R=0.72) and the slope (2.5 pptv/ppbv) agrees well with ratios from urban areas of the United States in 1999-2005 (2.4 pptv/ppbv) (Baker et al., 2008) as well as with charcoal burning emission ratios (Andreae and Merlet, 2001). The ARIAs emission ratio of benzene/CO (1.8 pptv/ppbv) is slightly higher than found in urban regions of the United States (0.7, Baker et al., 2008) and Mexico City (0.93-1.20, Apel et al., 2010), likely due to higher emissions by widespread combustion of coal and agricultural residues (Zhang et al., 2015). By contrast, the ARIAs emission ratios of ethylene and acetylene to CO (2.9. and 1.4 pptv/ppbv, respectively) are lower than observed in urban areas in the United States (4.1 and 3.4 pptv/ppbv, respectively) and Mexico City (7.90-8.40 and 8.20-9.60 pptv/ppbv, respectively), where the dominant source was reported to be transportation-related (Baker

et al., 2008). The lower ratio of ethylene/CO is comparable to emission ratios reported from charcoal burning (2.3 pptv/ppbv) (Andreae and Merlet, 2001).

Fig. 4: How many vertical profiles were flown over each of the four cities? The uniformly high NOy values from 0 to 3 km altitude over 3 of the cities are puzzling. In particular the uniformly high NOy values above 2300 m are in contrast to cleaner conditions at these altitudes as indicated by the CO mixing ratios. In contrast, over the home airport near Shijiazhuang the NOy measurements show a much wider range of mixing ratios throughout the altitude range of the flights. How consistent were the NOy measurements throughout the deployment?

We thank the referee for bringing this question to our attention. There were 34 profiles over Shijiazhuang, 20 over Xingtai, 16 over Julu, and 7 over Quzhou. As stated in the caption of Figure 2, the total number of NO/NOy observations above 2500 m is small (~30 minutes total of measurements) since the instrument switched between NO and NOy at 10 s intervals and could not measure both species simultaneously. The NOy converter required lots of power, so we did not turn on the instrument on frequently.

The caption of Figure 4 denotes the data is 1-second observations, but the 1-minute version was used accidentally. For the 1-minute average data, Shijiazhuang has the most measurements above 2500 m (20-40 data points in each bin above this altitude) since we regularly conducted profiles at the beginning and end of each flight. The other spiral locations have less than 10 1-minute average data points (and usually less than 5 in two of the three locations). When the 1-second data is used, there is ~1500 data points in each bin over Shijiazhuang, while the other spiral locations generally have less than 400 data points. To avoid overinterpretation of the limited NO/NOy observations over the other three spiral locations, we will cut off the profiles at 2500 m for NO and NOy over Xingtai, Quzhou, and Julu.

We will add the following sentence to Section 2.1 of the revised manuscript:

> We remove observations of NO/NO_y over three spiral locations due to limited measurements.

We have removed the following phrase after "Median profiles of NOy below 500m are highest over Julu (27.6 ppbv)" from Section 3.1 to avoid overinterpretation of the limited high altitude NO/NOy measurements:

> while aloft concentrations are similar between the spiral locations (~13 ppbv between 2500-3000 m).

Figure 4 will be updated as shown below, removing the high-altitude NOy measurements from the three spiral locations, with the updated figure caption reading:

> Figure 4. Vertical profiles of 1-second NO (red), NO_2 (blue), NO_y (green), CO (orange), and O_3 (purple) in 500 m bins over the 4 spiral locations: Xingtai (a), Shijiazhuang (b), Quzhou (c), and Julu (d). The dashed lines indicate the 10^{th} and 90^{th} percentiles, the solid

line is the median and the dotted line is the mean. We remove observations of NO/NOy above 2500 m over three spiral locations due to limited measurements.

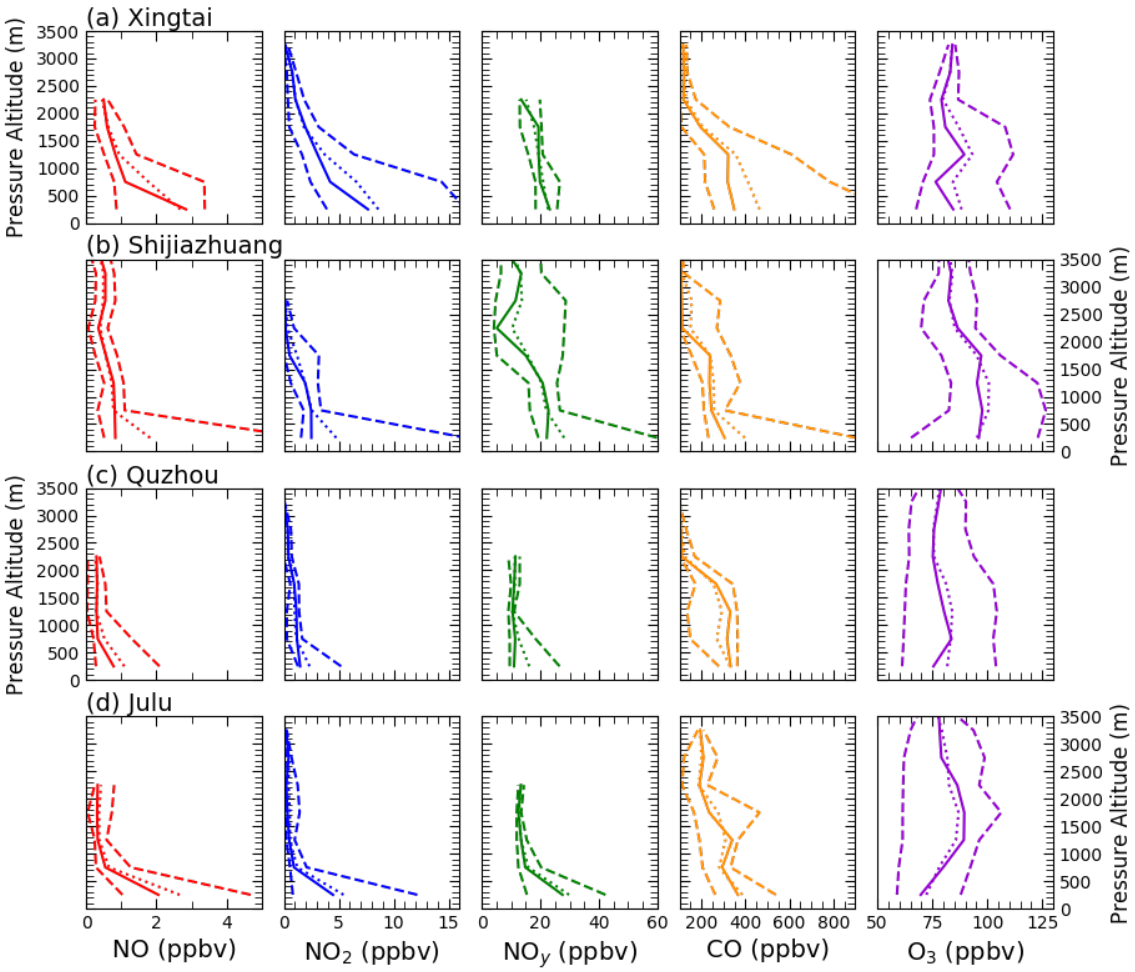

The instantaneous O3 production rate and the VOC or NOx limitation: As intense city or power plant plumes age and mixing with the surrounding air during transport, the photochemical ozone production tends to transition from being more VOC to more NOx limited. To capture these transitions and adjustments with a photochemical box model is challenging and is not captured by running the box model simply for 3 days as done in the present paper (line 143). How was the photochemical box model run for the present study? Were the j-values held constant or was their diurnal cycle taken into account?

We apologize for the confusion in the description of the box modeling simulations. The idea is that a spectrum of fresh and aged air parcels were observed and modeled. The box model was

run for seven ARIAs flights. On the days that a flight occurred, a surface simulation was also run. The three days as referenced in line 143 of the original paper were intended to describe the number of days the model was run in solar cycle mode. In the solar cycle configuration, the model allows the solar zenith angle to evolve in "real time" over the course of a model step. Photolysis frequencies, not measured during ARIAs or at the A^2BC supersite, evolve over the course of a model step and are calculated by combining cross sections and quantum yields with solar spectra derived from the NCAR Tropospheric Ultraviolet and Visible (TUV) version 5.2 radiation model. These agree within experimental error with direct measurements (Shetter et al., 2003). At the start of the model run, input solar zenith angle, altitude or elevation, O_3 column, and surface albedo are used for linear interpolation across TUV lookup tables (F0AM's "hybrid" method). We use SZA and altitude/elevation from ARIAs/A^2BC measurements and constant values for ozone column (325 DU) and surface albedo (0.17), which we estimate based on concurrent data from the OMI level-3 OMDOAO3e data product. We have expanded the methods Section 2.2 to more clearly explain how the photochemical box model was run. The revised Section 2.2 text will read as follows:

> A box model called Framework in 0-Dimensional Atmospheric Modelling (F0AMv3.1) (Wolfe et al., 2016) is used to evaluate oxidation processes to understand O_3 photochemical production both at the surface and aloft. The box model simulations cover the Y-12 flight tracks during seven flights and daytime hours at the A^2BC supersite in Xingtai (where the Y-12 conducted spirals) using the Carbon Bond Mechanism, version 6, revision 2 (CB6r2). Both the Y-12 flights and surface simulations define a physical loss lifetime of 24 hours to mitigate build-up of long-lived oxidation products over multiple days of integration.
>
> For the ARIAs flight data, the model is constrained by 1-minute average observed concentrations of VOCs, NO_2, CO, and O_3. Due to the limited number of grab canisters per flight, VOCs are constrained based on the altitude of the sampling relative to the height of the PBL, which is determined using potential temperature and water vapor vertical profiles for each flight. All WAS canister data collected below the top of the PBL during a flight are averaged. Data from all of the WAS canisters for the entire campaign collected above the research flight's PBL are averaged for that flight. Periodic missing Y-12 NO_2 data due to internal auto-zeroing are linearly interpolated since gaps were short (~2 minutes). The chemical system defined by each set of observations is integrated 5 days forward in time, in 1-hour time steps with diurnal variation of solar zenith angle (SZA), in order for calculated reactive intermediates to achieve diel steady state. Reaction rate constants are calculated using aircraft measurements of pressure, temperature, and relative humidity. The SZA is determined based on the time and location of the aircraft, and used to calculate photolysis rates as described below.
>
> For the A^2BC surface data, the model is constrained by 5-minute average concentrations of VOCs, NO_2, CO, and O_3 on days that a flight occurred. For May 17, surface data for NO_2 is filled with 1-hour average data collected for other days of the month, due to missing surface measurements on this day. The average concentrations from the WAS canisters below 500 m are used as ground concentrations since A^2BC did not measure VOCs at the surface. Similar to the flight data, the chemical system for the surface observations is integrated for 3 days forward in time, in 1-hour time steps with time-varying SZA, to reach diel steady state. Reaction rate constants are calculated from

ground measurements of pressure, temperature, and relative humidity. Time and ground elevation are used to calculate the SZA, which controls photolysis frequencies as described below.

Photolysis frequencies, not measured during ARIAs or at the A^2BC supersite, evolve over the course of a model step and are calculated by combining cross sections and quantum yields with solar spectra derived from the NCAR Tropospheric Ultraviolet and Visible (TUV) version 5.2 radiation model. At the start of the model run, input solar zenith angle, altitude or elevation, O_3 column, and surface albedo are used for linear interpolation across TUV lookup tables (F0AM's "hybrid" method). We use SZA and altitude/elevation from ARIAs/A^2BC measurements and constant values for ozone column (325 DU) and surface albedo (0.17), which we estimate based on concurrent data from the OMI level-3 OMDOAO3e data product (**https://disc.gsfc.nasa.gov/datasets/OMDOAO3e_003/summary?keywords=OMDOAO3e_003**). A correction factor of 0.8, determined by trial and error, is used to scale j-values to better agree with the observed NO/NO_2 ratio.

The impact of aerosols on O_3 production depends on the optical properties as well as the vertical distribution (Dickerson et al., 1997; Kelley et al., 1995). In the presence of scattering and absorbing aerosols, photolysis frequencies will be altered, thus changing the O_3 formation and atmospheric oxidizing capability (Wu et al., 2020a). Previous research over China has shown that as AOD increases, the extinction effect of aerosols on photolysis frequencies decreases due to a higher proportion of scattering aerosols under high AOD conditions (Wang et al., 2019a). Optical depth, single scattering albedo, and angstrom exponent during ARIAs (see Wang et al., 2018a) are used in the TUV online calculator (**https://cprm.acom.ucar.edu/Models/TUV/Interactive_TUV/**) to assess the impact of aerosols on photolysis frequencies. Most of the aerosol particles during ARIAs were concentrated in the lowest 2 km of the atmosphere with a single scattering albedo at 550 nm of 0.85 and an average AOD ~0.2. The impact of aerosol optical properties measured during ARIAs on photolysis frequencies is small compared to the default setting, so no additional adjustments are made to the model values.

The method described here to constrain VOCs introduces large uncertainty due to the sparsity of measurements obtained over a large area that potentially consists of a wide variety of chemical compositions. However, the production of O_3 aloft is not well characterized over Hebei, so our observations may help improve the understanding of air pollution for this region, despite this limitation. Additionally, unlike a 3-dimensional chemical transport model, the box model simulations do not include advection or emissions. These processes, while important, are not included in the box model since O_3 precursors were measured and used to constrain the box model calculations. Box modelling is used to gain an understanding of O_3 production and its sensitivity to ambient levels of NO_x and VOCs based upon measured meteorological parameters and the concentration of a wide variety of chemical species.

References (new with *):

*An, Z., Huang, R. J., Zhang, R., Tie, X., Li, G., Cao, J., Zhou, W., Shi, Z., Han, Y., Gu, Z. and

Ji, Y.: Severe haze in northern China: A synergy of anthropogenic emissions and atmospheric processes, Proc. Natl. Acad. Sci. U. S. A., 116(18), 8657–8666, doi:10.1073/pnas.1900125116, 2019.

Andreae, M. O. and Merlet, P.: Emission of trace gases and aerosols from biomass burning, Global Biogeochem. Cycles, 15(4), 955–966, doi:10.1029/2000GB001382, 2001.

*Apel, E. C., Emmons, L. K., Karl, T., Flocke, F., Hills, A. J., Madronich, S., Lee-Taylor, J., Fried, A., Weibring, P., Walega, J., Richter, D., Tie, X., Mauldin, L., Campos, T., Weinheimer, A., Knapp, D., Sive, B., Kleinman, L., Springston, S., Zaveri, R., Ortega, J., Voss, P., Blake, D., Baker, A., Warneke, C., Welsh-Bon, D., de Gouw, J., Zheng, J., Zhang, R., Rudolph, J., Junkermann, W. and Riemer, D. D.: Chemical evolution of volatile organic compounds in the outflow of the Mexico City Metropolitan area, Atmos. Chem. Phys., 10(5), 2353–2375, doi:10.5194/acp-10-2353-2010, 2010.

*Baker, A. K., Beyersdorf, A. J., Doezema, L. A., Katzenstein, A., Meinardi, S., Simpson, I. J., Blake, D. R. and Sherwood Rowland, F.: Measurements of nonmethane hydrocarbons in 28 United States cities, Atmos. Environ., 42(1), 170–182, doi:10.1016/j.atmosenv.2007.09.007, 2008.

*Cao, G., Zhang, X., Gong, S. and Zheng, F.: Investigation on emission factors of particulate matter and gaseous pollutants from crop residue burning, J. Environ. Sci., 20(1), 50–55, doi:10.1016/S1001-0742(08)60007-8, 2008.

*Di Carlo, P., Brune, W. H., Martinez, M., Harder, H., Lesher, R., Ren, X., Thornberry, T., Carroll, M. A., Young, V., Shepson, P. B., Riemer, D., Apel, E. and Campbell, C.: Missing OH Reactivity in a Forest: Evidence for Unknown Reactive Biogenic VOCs, Science (80-.)., 304(5671), 722–725, doi:10.1126/science.1094392, 2004.

*Dickerson, R. R., Kondragunta, S., Stenchikov, G., Civerolo, K. ., Doddridge, B. G. and Holben, B. N.: The Impact of Aerosols on Solar Ultraviolet Radiation and Photochemical Smog, Science (80-.)., 278(5339), 827–830, doi:10.1126/science.278.5339.827, 1997.

*Fan, H., Zhao, C. and Yang, Y.: A comprehensive analysis of the spatio-temporal variation of urban air pollution in China during 2014–2018, Atmos. Environ., 220(October 2019), 117066, doi:10.1016/j.atmosenv.2019.117066, 2020.

*Gaubert, B., Emmons, L. K., Raeder, K., Tilmes, S., Miyazaki, K., Jr, A. F. A., Elguindi, N., Granier, C., Tang, W., Barré, J., Worden, M., Buchholz, R. R., Edwards, D. P., Franke, P. and Anderson, J. L.: Correcting model biases of CO in East Asia : impact on oxidant distributions during KORUS-AQ, Atmos. Chem. Phys. Discuss. [online] Available from: https://doi.org/10.5194/acp-2020-599, 2020.

*Guo, S., Hu, M., Zamora, M. L., Peng, J., Shang, D., Zheng, J., Du, Z., Wu, Z., Shao, M., Zeng, L., Molina, M. J. and Zhang, R.: Elucidating severe urban haze formation in China, Proc. Natl. Acad. Sci. U. S. A., 111(49), 17373–17378, doi:10.1073/pnas.1419604111, 2014.

Halliday, H. S., Digangi, J. P., Choi, Y., Diskin, G. S., Pusede, S. E. and Rana, M.: Using Short - Term CO/CO_2 Ratios to Assess Air Mass Differences over the Korean Peninsula during KORUS - AQ, J. Geophys. Res. Atmos., 0–2, doi:10.1029/2018JD029697, 2019.

*Han, S., Kondo, Y., Oshima, N., Takegawa, N., Miyazaki, Y., Hu, M., Lin, P., Deng, Z., Zhao, Y., Sugimoto, N. and Wu, Y.: Temporal variations of elemental carbon in Beijing, J. Geophys. Res. Atmos., 114(23), 1–16, doi:10.1029/2009JD012027, 2009.

*Huang, M., Carmichael, G. R., Crawford, J. H., Wisthaler, A., Zhan, X., Hain, C. R., Lee, P. and Guenther, A. B.: Biogenic isoprene emissions driven by regional weather predictions using different initialization methods: Case studies during the SEAC4RS and DISCOVER-AQ airborne campaigns, Geosci. Model Dev., 10(8), 3085–3104, doi:10.5194/gmd-10-3085-2017, 2017.

*Huang, X., Wang, T., Talbot, R., Xie, M., Mao, H., Li, S., Zhuang, B., Yang, X., Fu, C., Zhu, J., Huang, X. and Xu, R.: Temporal characteristics of atmospheric CO2 in urban Nanjing, China, Atmos. Res., 153, 437–450, doi:10.1016/j.atmosres.2014.09.007, 2015.

*Kelley, P., Dickerson, R. R., Luke, T. and Kok, G. L.: Rate of NO_2 photolysis from the surface to 7.6 km altitude in clear-sky and clouds, Geophys. Res. Let., 22(19), 2621–2624, 1995.

Li, L., Xie, S., Zeng, L., Wu, R. and Li, J.: Characteristics of volatile organic compounds and their role in ground-level ozone formation in the Beijing-Tianjin-Hebei region, China, Atmos. Environ., 113, 247–254, doi:10.1016/j.atmosenv.2015.05.021, 2015.

*Li, L. Y., Chen, Y. and Xie, S. D.: Spatio-temporal variation of biogenic volatile organic compounds emissions in China, Environ. Pollut., 182, 157–168, doi:10.1016/j.envpol.2013.06.042, 2013.

*Liu, H., Jacob, D. J., Bey, I., Yantosca, R. M., Duncan, B. N. and Sachse, G. W.: Transport pathways for Asian pollution outflow over the Pacific: Interannual and seasonal variations, J. Geophys. Res. D Atmos., 108(20), doi:10.1029/2002jd003102, 2003.

*Ma, M., Gao, Y., Wang, Y., Zhang, S., Ruby Leung, L., Liu, C., Wang, S., Zhao, B., Chang, X., Su, H., Zhang, T., Sheng, L., Yao, X. and Gao, H.: Substantial ozone enhancement over the North China Plain from increased biogenic emissions due to heat waves and land cover in summer 2017, Atmos. Chem. Phys., 19(19), 12195–12207, doi:10.5194/acp-19-12195-2019, 2019.

*Mo, Z., Shao, M., Wang, W., Liu, Y., Wang, M. and Lu, S.: Evaluation of biogenic isoprene emissions and their contribution to ozone formation by ground-based measurements in Beijing, China, Sci. Total Environ., 627, 1485–1494, doi:10.1016/j.scitotenv.2018.01.336, 2018.

*Peterson, D. A., Hyer, E. J., Han, S. O., Crawford, J. H., Park, R. J., Holz, R., Kuehn, R. E., Eloranta, E., Knote, C., Jordan, C. E. and Lefer, B. L.: Meteorology influencing springtime air

quality, pollution transport, and visibility in Korea, Elementa, 7(1), doi:10.1525/elementa.395, 2019.

Pusede, S. E., Gentner, D. R., Wooldridge, P. J., Browne, E. C., Rollins, A. W., Min, K. E., Russell, A. R., Thomas, J., Zhang, L., Brune, W. H., Henry, S. B., Digangi, J. P., Keutsch, F. N., Harrold, S. A., Thornton, J. A., Beaver, M. R., St. Clair, J. M., Wennberg, P. O., Sanders, J., Ren, X., Vandenboer, T. C., Markovic, M. Z., Guha, A., Weber, R., Goldstein, A. H. and Cohen, R. C.: On the temperature dependence of organic reactivity, nitrogen oxides, ozone production, and the impact of emission controls in San Joaquin Valley, California, Atmos. Chem. Phys., 14(7), 3373–3395, doi:10.5194/acp-14-3373-2014, 2014.

*Ren, X., Salmon, O. E., Hansford, J. R., Ahn, D., Hall, D., Benish, S. E., Stratton, P. R., He, H., Sahu, S., Grimes, C., Heimburger, A. M. F., Martin, C. R., Cohen, M. D., Stunder, B., Salawitch, R. J., Ehrman, S. H., Shepson, P. B. and Dickerson, R. R.: Methane Emissions from the Baltimore-Washington Area Based on Airborne Observations: Comparison to Emissions Inventories, J. Geophys. Res. Atmos., 1–14, doi:10.1029/2018JD028851, 2018.

*Seinfeld, J. H. and Pandis, S. N.: Atmospheric Chemsitry and Physics, 2nd ed., John Wiley & Sons, Inc., New Jersey., 2006.

*Shetter, R. E., Junkermann, W., Swartz, W. H., Frost, G. J., Crawford, J. H., Lefer, B. L., Barrick, J. D., Hall, S. R., Hofzumahaus, A., Bais, A., Calvert, J. G., Cantrell, C. A., Madronich, S., Müller, M., Kraus, A., Monks, P. S., Edwards, G. D., McKenzie, R., Johnston, P., Schmitt, R., Griffioen, E., Krol, M., Kylling, A., Dickerson, R. R., Lloyd, S. A., Martin, T., Gardiner, B., Mayer, B., Pfister, G., Röth, E. P., Koepke, P., Ruggaber, A., Schwander, H. and van Weele, M.: Photolysis frequency of NO2: Measurement and modeling during the International Photolysis Frequency Measurement and Modeling Intercomparison (IPMMI), J. Geophys. Res. Atmos., 108(16), doi:10.1029/2002jd002932, 2003.

*Si, Y., Wang, H., Cai, K., Chen, L., Zhou, Z. and Li, S.: Long-term (2006–2015) variations and relations of multiple atmospheric pollutants based on multi-remote sensing data over the North China Plain, Environ. Pollut., 255, 113323, doi:10.1016/j.envpol.2019.113323, 2019.
Silva, S. J., Arellano, A. F. and Worden, H. M.: Toward anthropogenic combustion emission constraints from space-based analysis of urban CO2/CO sensitivity, Geophys. Res. Lett., 40(18), 4971–4976, doi:10.1002/grl.50954, 2013.

*Souri, A., Nowlan, C., González Abad, G., Zhu, L., Blake, D., Fried, A., Weinheimer, A., Woo, J.-H., Zhang, Q., Chan Miller, C., Liu, X. and Chance, K.: An Inversion of NOx and NMVOC Emissions using Satellite Observations during the KORUS-AQ Campaign and Implications for Surface Ozone over East Asia, Atmos. Chem. Phys., 1(x), 1–39, doi:10.5194/acp-2020-220, 2020.

*Tang, W., Arellano, A. F., DiGangi, J. P., Choi, Y., Diskin, G. S., Agustí-Panareda, A., Parrington, M., Massart, S., Gaubert, B., Lee, Y., Kim, D., Jung, J., Hong, J., Hong, J. W., Kanaya, Y., Lee, M., Stauffer, R. M., Thompson, A. M., Flynn, J. H. and Woo, J. H.: Evaluating high-resolution forecasts of atmospheric CO and CO2 from a global prediction system during

KORUS-AQ field campaign, Atmos. Chem. Phys., 18(15), 11007–11030, doi:10.5194/acp-18-11007-2018, 2018.

*Tang, W., Worden, H. M., Deeter, M. N., Edwards, D. P., Emmons, L. K., Martínez-Alonso, S., Gaubert, B., Buchholz, R. R., DIskin, G. S., DIckerson, R. R., Ren, X., He, H. and Kondo, Y.: Assessing Measurements of Pollution in the Troposphere (MOPITT) carbon monoxide retrievals over urban versus non-urban regions, Atmos. Meas. Tech., 13(3), 1337–1356, doi:10.5194/amt-13-1337-2020, 2020.

Wang, F., Li, Z., Ren, X., Jiang, Q., He, H., Dickerson, R. R., Dong, X. and Lv, F.: Vertical distributions of aerosol optical properties during the spring 2016 ARIAs airborne campaign in the North China Plain, Atmos. Chem. Phys. Discuss., (January), 1–22, doi:10.5194/acp-2017-1021, 2018.

*Wang, Q., Han, Z., Wang, T. and Zhang, R.: Impacts of biogenic emissions of VOC and NOx on tropospheric ozone during summertime in eastern China, Sci. Total Environ., 395(1), 41–49, doi:10.1016/j.scitotenv.2008.01.059, 2008.

*Wang, W., Li, X., Shao, M., Hu, M., Zeng, L., Wu, Y. and Tan, T.: The impact of aerosols on photolysis frequencies and ozone production in Beijing during the 4-year period 2012 – 2015, Atmos. Chem. Phys., (2), 9413–9429, 2019a.

*Wang, Y., Munger, J. W., Xu, S., McElroy, M. B., Hao, J., Nielsen, C. P. and Ma, H.: CO2 and its correlation with CO at a rural site near Beijing: Implications for combustion efficiency in China, Atmos. Chem. Phys., 10(18), 8881–8897, doi:10.5194/acp-10-8881-2010, 2010.

Wang, Y., Dörner, S., Donner, S., Böhnke, S., Smedt, I., Dickerson, R. R., Dong, Z., He, H., Li, Z., Li, Z., Li, D., Liu, D., Ren, X., Theys, N., Wang, Y., Wang, Y., Wang, Z., Xu, H., Xu, J. and Wagner, T.: Vertical profiles of NO2, SO2, HONO, HCHO, CHOCHO and aerosols derived from MAX-DOAS measurements at a rural site in the central western North China Plain and their relation to emission sources and effects of regional transport, Atmos. Chem. Phys, (2), 5417–5449, 2019b.

*Warneke, C., McKeen, S. A., de Gouw, J. A., Goldan, P. D., Kuster, W. C., Holloway, J. S., Williams, E. J., Lerner, B. M., Parrish, D. D., Trainer, M., Fehsenfeld, F. C., Kato, S., Atlas, E. L., Baker, A. and Blake, D. R.: Determination of urban volatile organic compound emission ratios and comparison with an emissions database, J. Geophys. Res. Atmos., 112(10), doi:10.1029/2006JD007930, 2007.

Wolfe, G. M., Marvin, M. R., Roberts, S. J., Travis, K. R. and Liao, J.: The framework for 0-D atmospheric modeling (F0AM) v3.1, Geosci. Model Dev., 9(9), 3309–3319, doi:10.5194/gmd-9-3309-2016, 2016.

*Wu, J., Bei, N., Hu, B., Liu, S., Wang, Y., Shen, Z., Li, X., Liu, L., Wang, R., Liu, Z., Cao, J., Tie, X., Molina, L. T. and Li, G.: Aerosol–photolysis interaction reduces particulate matter during wintertime haze events, Proc. Natl. Acad. Sci. U. S. A., 117(18), 9755–9761,

doi:10.1073/pnas.1916775117, 2020a.

*Wu, K., Yang, X., Chen, D., Gu, S., Lu, Y., Jiang, Q., Wang, K., Ou, Y., Qian, Y., Shao, P. and Lu, S.: Estimation of biogenic VOC emissions and their corresponding impact on ozone and secondary organic aerosol formation in China, Atmos. Res., 231(April 2019), 104656, doi:10.1016/j.atmosres.2019.104656, 2020b.

*Xia, L., Zhang, G., Liu, L., Li, B., Zhan, M., Kong, P. and Wang, H.: Atmospheric CO2 and CO at Jingdezhen station in central China: Understanding the regional transport and combustion efficiency, Atmos. Environ., 222(July 2019), 117104, doi:10.1016/j.atmosenv.2019.117104, 2020.

*Xue, L., Wang, T., Simpson, I. J., Ding, A., Gao, J., Blake, D. R., Wang, X., Wang, W., Lei, H. and Jin, D.: Vertical distributions of non-methane hydrocarbons and halocarbons in the lower troposphere over northeast China, Atmos. Environ., 45(36), 6501–6509, doi:10.1016/j.atmosenv.2011.08.072, 2011.

*Zhang, Z., Wang, X., Zhang, Y., Lü, S. and Huang, Z.: Ambient air benzene at background sites in China's most developed coastal regions : Exposure levels , source implications and health risks, Sci. Total Environ., 511, 792–800, doi:10.1016/j.scitotenv.2015.01.003, 2015.

*Zong, R., Yang, X., Wen, L., Xu, C., Zhu, Y., Chen, T., Yao, L., Wang, L., Zhang, J., Yang, L., Wang, X., Shao, M., Zhu, T., Xue, L. and Wang, W.: Strong ozone production at a rural site in the North China Plain: Mixed effects of urban plumes and biogenic emissions, J. Environ. Sci. (China), 71, 261–270, doi:10.1016/j.jes.2018.05.003, 2018.